



Power Electronic Systems
Laboratory

© 2014 IEEE

Proceedings of the International Power Electronics Conference - ECCE Asia (IPEC 2014), Hiroshima, Japan, May 18-21, 2014

High-Speed Magnetically Levitated Reaction Wheel Demonstrator

C. Zwyssig,
T. Baumgartner,
J. W. Kolar

This material is published in order to provide access to research results of the Power Electronic Systems Laboratory / D-ITET / ETH Zurich. Internal or personal use of this material is permitted. However, permission to reprint/republish this material for advertising or promotional purposes or for creating new collective works for resale or redistribution must be obtained from the copyright holder. By choosing to view this document, you agree to all provisions of the copyright laws protecting it.



Eidgenössische Technische Hochschule Zürich
Swiss Federal Institute of Technology Zurich

High-Speed Magnetically Levitated Reaction Wheel Demonstrator

Christof Zwyssig
Celeroton Ltd.
Zurich, Switzerland
christof.zwyssig@celeroton.com

Thomas Baumgartner
Celeroton Ltd.
Zurich, Switzerland
thomas.baumgartner@celeroton.com

Johann W. Kolar
Power Electronic Systems Laboratory
ETH Zurich
Zurich, Switzerland
kolar@lem.ee.ethz.ch

Abstract— Reaction wheels (RWs) for small satellites with active magnetic bearings allowing for ultra-high-speed operation show advantages in angular momentum density over ball bearing RWs with limited speed according to scaling laws developed in this paper. A reaction wheel demonstrator design based on a novel dual hetero-/homopolar, slotless, self-bearing, permanent-magnet synchronous motor concept with a rotational speed of 250 000 rpm is investigated. The design includes the rotor dynamics, mechanical stress analysis, electromagnetics, power electronics and control, and the sensor concept. The experimental setup ready for experimental verification is presented.

Keywords— reaction wheel, self-bearing, active magnetic bearing, high-speed.

I. INTRODUCTION

Single reaction wheels (RWs), 3 or more RWs combined into reaction wheel assemblies (RWAs) or integrated power and attitude control systems (IPACS) using an RWA also for energy storage, are used for attitude control of satellites in orbit flight. Changes in rotational speed vary the angular momentum of an RW, which causes the spacecraft to counter-rotate through conservation of total angular momentum. Usually, ball bearings are employed in RWs [1], but also magnetic bearing reaction wheels have been developed, usually for larger satellites, in a few cases also for smaller satellites [2]. If an RW for small spacecrafts is designed, typically, the maximum rotor diameter is limited. Thus, a very high rotational speed has to be selected to maximize the angular momentum (and energy storage capacity in case of IPACS). Today, the maximum rotational speed is typically limited by the employed bearings and the required lifetime, to typically 5 000 to 10 000 rpm, also in the case of magnetic bearings.

Therefore, in this paper a RW demonstrator for small satellites based on a high-speed, magnetically levitated electrical drive system is presented, which allows to increase the rotational speed from currently achieved 10 000 rpm to over 200 000 rpm.

First, RW requirements and scaling laws are identified, showing that the only way to higher performance density RWs is an increase in rotational speed. Then, the electromagnetic concept and design based on two different slotless self-bearing motors, a heteropolar and a homopolar motor, is described in detail. The main aspects of the mechanical design, the stress analysis and rotordynamic design, are also presented. Finally, the experimental setup including reaction wheel demonstrator and power and control electronics is shown and first measurement results are presented.

II. REACTION WHEEL REQUIREMENTS AND SCALING

Most space vehicles designed today require some form of attitude control. Some typical applications are:

- Orientation of solar arrays
- Orientation of optical payloads such as telescopes
- Orientation of scientific instruments
- Orientation of high gain antennas to a ground based station or another spacecraft
- Orientation of orbit thrusters

A typical attitude system consists of an attitude measurement system, a control algorithm and a set of RWs. The measurement system is used to determine the actual attitude. The control algorithm compares the actual attitude with the desired attitude and determines the control input to obtain the desired attitude. Finally, the RWs apply the control torque to the spacecraft.

The design of an attitude control system is mainly determined by the space mission requirements such as the accuracy and stability of the attitude control, the spacecraft's mass and the nature of disturbance torques. Since the functionality of the attitude control system is essential for the overall space mission, the lifetime of the control actuators is crucial. Typical design lifetimes of satellites are 5 to 15 years [3]. Therefore, if using ball bearings, the actuators speeds are limited to around 10 000 rpm.

A. Reaction disk scaling laws

When the reaction disk is operated at the stress limitation (optimal operation conditions), the angular momentum L (which is the main RW performance criterion) can be expressed by

$$L = I\omega = \frac{1}{2}m_{rotor}r^2\omega = \frac{1}{2}\pi\rho\frac{r^5}{x}\omega$$

$$= \pi\sqrt{\frac{2}{3+\nu}}\sqrt{\sigma_{max}\rho}\cdot\frac{r^4}{x} \quad (1)$$

where I is the inertia, ω the angular rotational speed, m_{rotor} the weight, r the radius, x the factor of radius to length, ρ the density, ν the Poisson's ratio, and σ_{max} the tensile strength of the inertia disk material.

From this it can be seen that if L is to be maximized, the radius r has to be selected as large as possible. For a given L , this results in a thin disk (small value of x). Typically, the maximum diameter of the rotor is limited by the geometrical constraints of the spacecraft and the rotor dynamical behavior. For fixed rotor proportions (constant x), all rotor dimensions scale according to above equation with

$$r \propto \sqrt[4]{L} \quad (2)$$

as a function of angular momentum storage capacity L . With this relationship, the rotor mass scaling can be derived to

$$m_{rotor} \propto \sqrt[4]{L^3} \quad (3)$$

This result indicates that the rotor mass does not scale linearly to the momentum capacity L , i.e. smaller reaction wheels feature less angular momentum per mass than bigger ones. This is one of the main limitations and challenges when designing reaction wheels for small spacecrafts as small reaction wheels intrinsically are less mass efficient. Therefore, an optimization of the momentum capacity per mass is essential, i.e. an operation at the stress limitation becomes increasingly important when decreasing spacecraft size to achieve an acceptable performance.

The fact that smaller reaction wheels feature lower momentum capacity per mass is also validated by the market study presented in [4].

In order to utilize the rotor material, the rotational speed has to be adapted to the size of the rotor, i.e. the rotational speed scales with

$$\omega \propto \frac{1}{\sqrt[4]{L}} \quad (4)$$

This means that reaction wheels which are designed for smaller angular momentum storage capacities have to be designed for a higher rotational speed.

B. Electrical machine scaling laws

Beside the high-inertia rotor also an electric machine is necessary to accelerate or decelerate the rotor. The size required for the machine is mainly given by the torque requirement of the attitude control system. The torque

density (torque T divided by machine volume $m_{machine}$) obtained from an electric machine is widely independent of its size and rotational speed [5]. Thus, a constant torque density and torque per machine mass can be assumed for the scaling

$$\frac{T}{m_{machine}} \propto const. \quad (5)$$

The machine power P can be derived by multiplying the torque with the rotational speed. Thus, the power density increases linearly with the rotational speed

$$\frac{P}{m_{machine}} \propto \omega \quad (6)$$

In most applications of electrical machines, the power P has to meet the requirements of the application. Thus, if the rotational speed and with it also the power density is increased, the system mass can be reduced. Therefore, a high rotational speed is desirable. If this machine scaling is applied to a RW and if the acceleration time

$$t_{acc} = \frac{L}{T} \quad (7)$$

is kept constant, a machine mass scaling linear to the angular momentum results

$$m_{machine} \propto L \quad (8)$$

Consequently, the mass ratio between the machine and the rotor scales to

$$\frac{m_{machine}}{m_{rotor}} \propto \sqrt[4]{L} \quad (9)$$

This means that for smaller reaction wheels the size of the machine decreases faster than the size of the rotor. The overall power of the system scales to

$$P \propto \sqrt[4]{L^3} \quad (10)$$

Consequently, small reaction wheels feature more power per angular momentum capacity than bigger ones. Based on this scaling law, it can be concluded that a high rotational speed is especially desirable for RW used in IPACS since high power densities can be achieved.

C. Bearing requirements

All RWs RWAs and IPACS require bearings to support the rotor. The bearings are a critical part as they influence the RW design and limit performance of the RW. Critical bearing specifications are:

- Rotational speed of the rotor
- Lifetime
- Weight and inertias of the rotor
- Load transmission
- Size and weight of the bearing
- Atmosphere requirements

Most RWs employ ball bearings because of simplicity, compactness, low weight and high bearing load capability. However, ball bearings show a limited lifetime depending on rotational speed and lubricant life

[6]. In section II.A it is derived that smaller angular momentum (L) RWs show in lower angular momentum density (L/m), and the only way to counteract and optimize this (to increase L/m) is to increase the rotational speed. As a consequence, the ball bearing becomes an increasing challenge, and is usually defining the performance limit, in small RWs. A further disadvantage of ball bearings is they usually require a pressurized atmosphere to prevent outgassing of the lubricant, and therefore containment is required.

To overcome the limitations and drawbacks of ball bearings at high rotational speeds and vacuum requirement, a novel magnetically levitated high-speed machine has been developed in [7]. This is the basis of RW demonstrator presented in this paper.

D. Summary of scaling laws

RWs employing ball bearings are compared to magnetically levitated RWs based on the high-speed, slotless, self-bearing, permanent-magnet synchronous machine presented in [7]. The total system mass (including machine, electronics, housing, etc.) is calculated based on realistic reference designs for ball bearing RWs and for the high-speed self-bearing machine. Both systems employ the same reaction disk shape, machine model (mass proportional to torque), power electronics model (mass proportional to power), and a constant acceleration time of 20 s is assumed. The control electronics are constant in both systems, however the mass of the self-bearing control is much higher than the ball bearing control (only motor control needed here). The ball bearing RW rotational speed is limited to a (high) value of 8000 rpm.

The results of the system scaling are shown in Figure 1. In order to give a comparison with state of the art RW systems employing ball bearings, typical reference designs are also shown in the total mass plot. For this, the systems RW1, RW35, RW90 and RW150 from Astro-und Feinwerktechnik Adlershof GmbH [8], which feature a similar acceleration time, are added to the plot. The total mass plot shown in Figure 1 shows that the mass of the commercially available systems is underestimated by approximately 20%. However, the general trend of the total mass versus the angular momentum is correctly rendered in the scaling. The red diamond shown in the plot shows the prototype system employing the machine presented in [7] when extended with a high inertia titanium reaction disk.

The comparison shows that above an angular momentum capacity of roughly 0.1 Nms (typical RW performance required in a satellite with total mass of 10-30 kg) the magnetically levitated system can be realized with a lower system mass. The mass saving is about 50% in the range of 1 Nms. Given the higher rotational speed and the identical torque requirement, the resulting power is much higher in the magnetically levitated system. This is a major disadvantage when used in an RWA, but a major advantage in IPACS because the RWs can be used as high power sources.

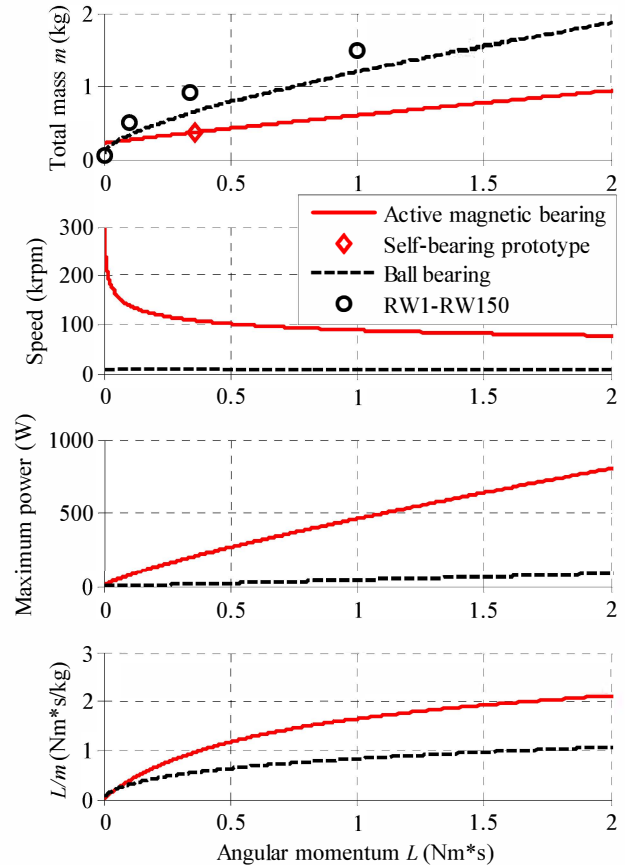


Figure 1: Reaction wheel system scaling. Typical RWs employing ball bearings are compared to RWs employing high-speed self-bearing motors. Additionally, commercially available systems employing ball bearings (RW1-RW150) are also shown for comparison.

III. REACTION WHEEL DEMONSTRATOR DESIGN

A. Dual hetero-/homopolar self-bearing motor concept

In the proposed novel dual hetero-/homopolar slotless self-bearing motor concept depicted in Figure 1, the bearing forces and drive torque are generated by two slotless, self-bearing, permanent-magnet synchronous motors employing an ironless rotor. Such slotless, self-bearing concepts have also been presented in [9] and [10]. There a disk motor (small length compared to diameter) with one active radial magnetic bearing and a passive stabilization of the tilting are utilized. Using disk motors for RWs would require integrating the permanent magnet(s) in the inertia disk. Because of the limited mechanical strength of magnets, the stress limited operation would be at much lower speeds than if a separate, high strength inertia disk can be used. In contrary to the disk motor concepts, the proposed demonstrator employs two individual self-bearing motors with two small rotor diameters in two active magnetic bearing parts instead of one large diameter disk motor. This separation of inertia disk and magnetic bearing allows integrating a specially designed reaction disk in between the two self-bearing motors and therefore going to stress limited operation at much higher rotational speeds –essential to realize RWs for small spacecraft.

A similar motor concept has also been presented in

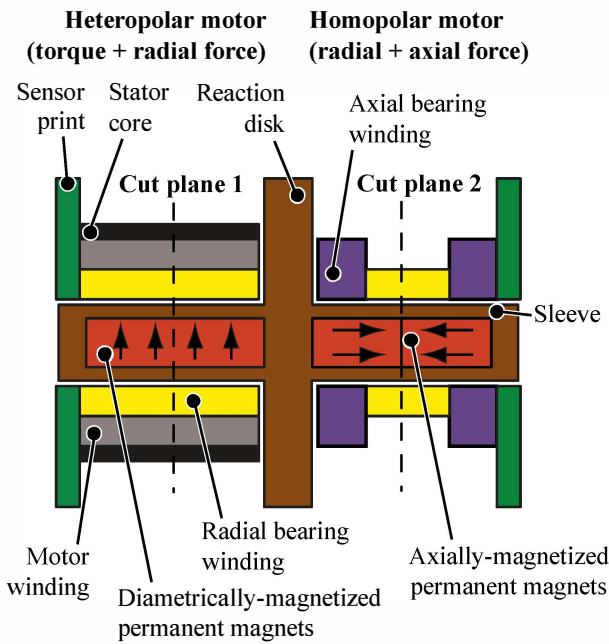


Figure 2: Novel dual hetero-/homopolar slotless self-bearing motor concept.

[7], where two heteropolar self-bearing motors, and an additional axially magnetized magnet plus an axial bearing coil control all six degrees of freedom. In contrary to this concept, the proposed demonstrator employs one heteropolar self-bearing motor (the same as in [7]) but replaces the second heteropolar self-bearing motor with a homopolar self-bearing motor. In the homopolar motor the radial bearing forces and the axial bearing force can be controlled with the same magnetic field generated by two axially magnetized magnets. This has the advantage that no extra magnet is required for the axial bearing force only, and the rotor can be made short for high bending modes, allowing high rotational speeds. Furthermore, in contrary to the concept in [7], the two motors are not placed right beside each other, but they are holding the application, in this case the inertia disk, from two ends. This is a further advantage concerning rotordynamics and further increases the first bending mode.

The application of forces and torque is divided up into the two motors: Motor torque and radial bearing forces are applied in the heteropolar motor, axial and radial bearing forces are applied in the homopolar motor. All six-degrees of freedom are controlled actively: The displacement in x - and y -direction, and the torque/tilting around the x - and y - axis is controlled by two radial bearings separated in z -direction (separated into the heteropolar motor and the homopolar motor). The torque around the z -axis is controlled by the heteropolar motor, the displacement in z -axis is controlled by the homopolar motor. The torque and force generation by Lorentz forces (by interaction of magnetic field and current) is explained in more detail in the following subsections.

The novel slotless self-bearing motor concept is completed with two PCB based eddy current displacement and hall effect rotation angle sensors. This

sensor concept has been presented in [11] and [7].

Compared to state-of-the-art reluctance type active magnetic bearings, this concept has various advantages allowing for high rotational speed such as

- Very short axial length and therefore shifting of bending modes to high frequencies
- Simple mechanical rotor construction resulting in low mechanical stresses at high speed
- Low high frequency losses due to slotless motor topology
- High force control bandwidth
- Feasible for miniaturization due to low mechanical complexity (especially on rotor side)

B. Electromagnetic force generation

1) Heteropolar motor

The force and torque generation is depicted in Figure 3, which is a cross section view of the cut plane 1 indicated in Figure 2. In the heteropolar motor the torque is generated with the motor winding sitting in between the bearing winding and the stator core. The motor winding has one pole-pair as the magnet. A first current in axial direction, together with a magnetic field in radial direction, leads to a force vector in azimuthal direction. Combining two currents in opposing axial directions displaced by 180° leads to a force pair that generates a torque vector in z -axis.

The bearing forces in x - and y - direction are generated by a bearing winding sitting between the air gap and the motor winding. The bearing winding has two pole-pairs, as for force generation the winding poles pair number has to be the rotor pole-pair number ± 1 . The four current vectors of a two pole-pair winding are displaced by 90° , and together with the magnetic field that changes angular direction every 90° as well this leads to forces in the same direction, leading to a bearing force e.g. in $-y$ direction.

The vast amount of generated torque and forces is based on Lorentz force generation, only a small, in the design negligible amount of reluctance force is present. The heteropolar slotless motor design and calculation of Lorentz based torque and forces with analytical models (and some FE calculations for reluctance forces) has been presented in [12] and [7] in detail. The same models and principles are used for the heteropolar motor in this paper. Therefore, linear relationships between the winding currents and the forces and torques are assumed.

2) Homopolar motor

The homopolar motor has two axially magnetized magnets pointing towards each other, and contains no back iron. This results in a field distribution as shown in Figure 4, which is homopolar, meaning there is no change in field if the rotor is rotating (assuming ideal isotropic conditions in the magnet and a fully concentric rotor design).

The axial force generation is depicted in Figure 4. The axial force is generated by two separate coils which are

wound in azimuthal turns around the rotor. The axial bearing coils are placed in a radius and z-location where they see mainly a radial magnetic field. This, together with the azimuthal currents, results in an axial force.

The radial force generation is depicted in Figure 5, which is a cross section view of the cut plane 2 indicated in Figure 2 and Figure 4. The radial forces are generated by a winding which essentially is the same as the motor winding of the heteropolar motor: a winding with one pole-pair sitting in between the axial bearing coils and also seeing mainly a radial field. The axial currents in opposing directions displaced by 180° , together with the homopolar field that changes angular direction also every 180° , leads to force vectors pointing in the same direction and therefore a bearing force e.g. in $-y$ direction.

For the homopolar motor, the generated torque and forces consists uniquely of Lorentz forces, therefore the equations and models in [12] and [7] can be applied for the homopolar motor in this paper, and all forces are proportional to current.

C. Specifications

The specifications for the RW demonstrator are not derived from a defined mission or satellite, but are chosen to allow for the verification of the feasibility of a RW based on the slotless, self-bearing permanent-magnet synchronous machine similar to the one firstly presented in [7]. Therefore, in this design, dimensions, rotational speed and motor torque are inputs parameters into the design, the angular momentum L , the acceleration time and the stored energy are results from the design. In a design for a defined satellite or mission, design input parameters would be resulting specifications, and vice versa results would be input parameters.

The machine described therein allows for rotational speeds up to 500 000 rpm. However, the rotational speed in a high-speed RW is limited by the stresses in the reaction disk. In the RW demonstrator presented in this paper, the reaction disk diameter is chosen to 48 mm, the

disk material is titanium grade 5. According to the mechanical stress calculation (Figure 6) this results in a maximum rotational speed of 250 000 rpm. The rotor length is chosen such that the first bending mode is approximately at double this maximal speed (Figure 7). This results in a total rotor length of 49 mm, of which 17 mm can be used for the heteropolar motor and 17 mm for the homopolar motor. The rotor diameter within the motors results from stress analysis of the permanent magnets and results in 8 mm.

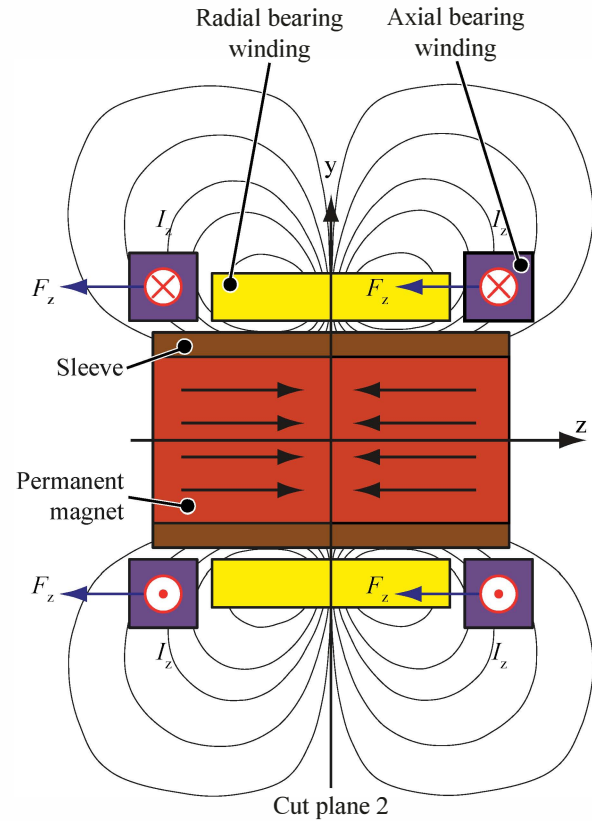


Figure 4: Axial force generation in the homopolar motor.

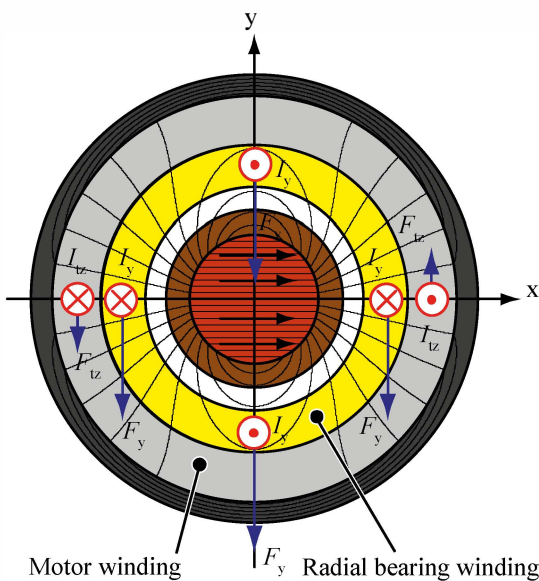


Figure 3: Torque and radial force generation in the heteropolar motor (cut plane 1 of Figure 2).

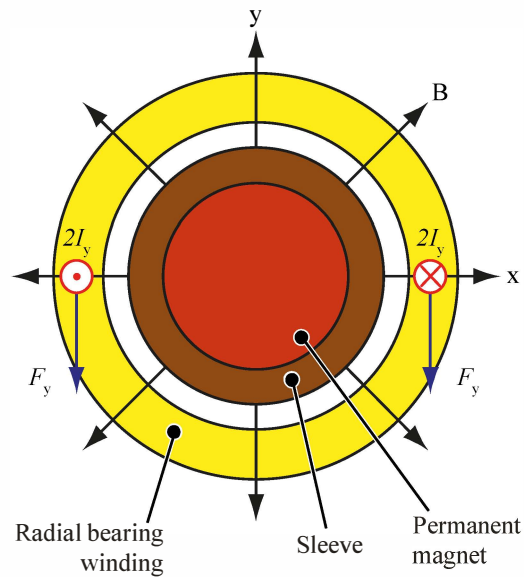


Figure 5: Radial force generation in the homopolar motor (cut plane 2 of Figure 2 and Figure 4).

This results in a rated motor torque of 7.8 Nmm, a maximal motor power of 345 W, an acceleration time of 45 s, a maximal angular momentum of 0.355 Nms, an and a maximal stored kinetic energy of 4.65 kJ. The motor back EMF, phase current and inverter signals for one phase of the motor at rated speed and power are depicted in Figure 8.

IV. EXPERIMENTAL VERIFICATION

A. Experimental Setup

Based on the concept and specifications presented in the previous sections, a demonstrator RW has been realized. In addition to the already presented parts in Figure 2 it consists of two motor casings where the heteropolar and the homopolar motor are built into, a central casing where these two motors are attached to including a holder, with which the entire setup can be mounted onto a baseplate. A photo of the demonstrator is shown in Figure 9.

In Figure 10, the power electronics to control the demonstrator are shown. The power electronics consist of two three-phase channels for the radial bearing windings, a single-phase channel for the axial bearing winding and a three-phase channel for the motor winding. It is controlled by a DSP/FPGA digital control platform, which also demodulates the rotor position sensor signals. The power electronics and control are similar to the system presented in [7] and [13].

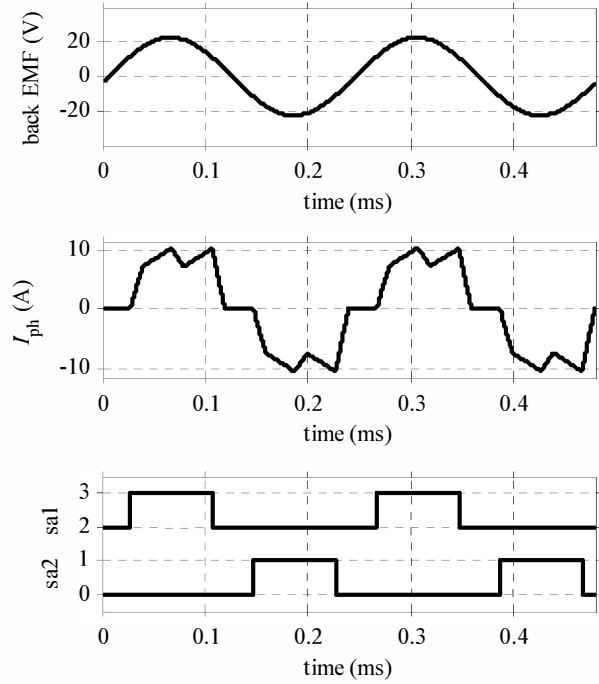


Figure 8: Simulated motor back EMF, phase current and PAM inverter switching signals for one phase at rated speed (250 000 rpm) and rated power (345 W).

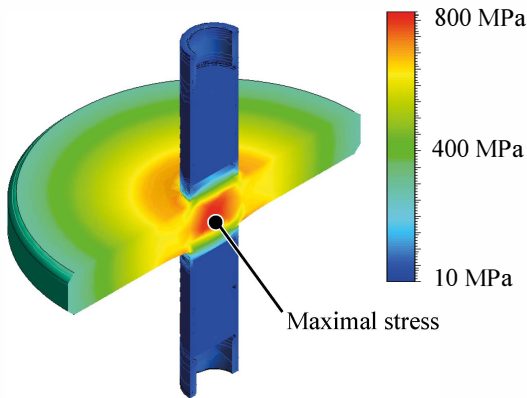


Figure 6: Mechanical stresses (von Mises) in the rotor at an overspeed of 250 000 rpm with the maximal stress of of 808 MPa in the center of the rotor.

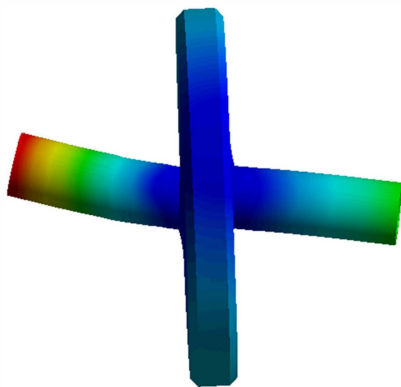


Figure 7: First bending mode of the rotor at 544 000 rpm.

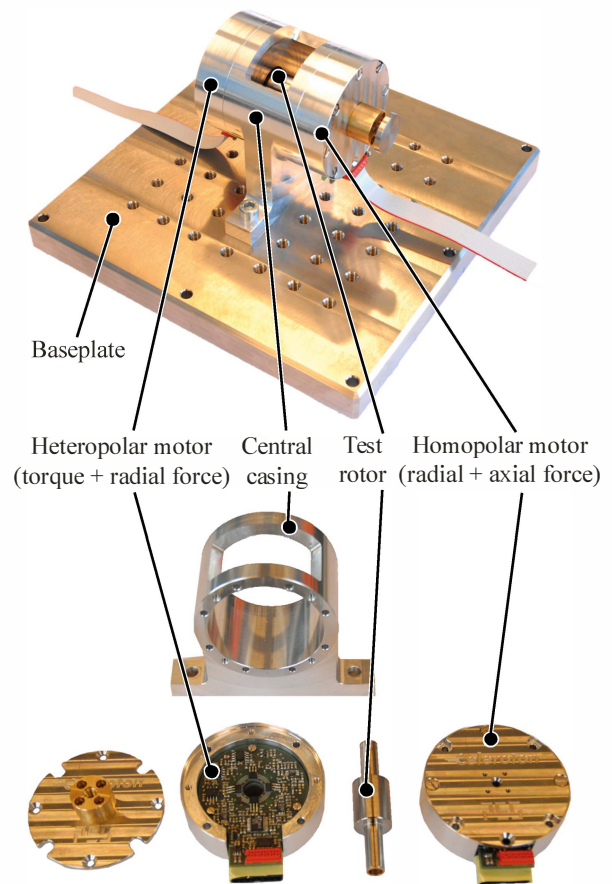


Figure 9: Novel dual hetero-/homopolar, slotless, self-bearing, permanent-magnet synchronous machine reaction wheel demonstrator.

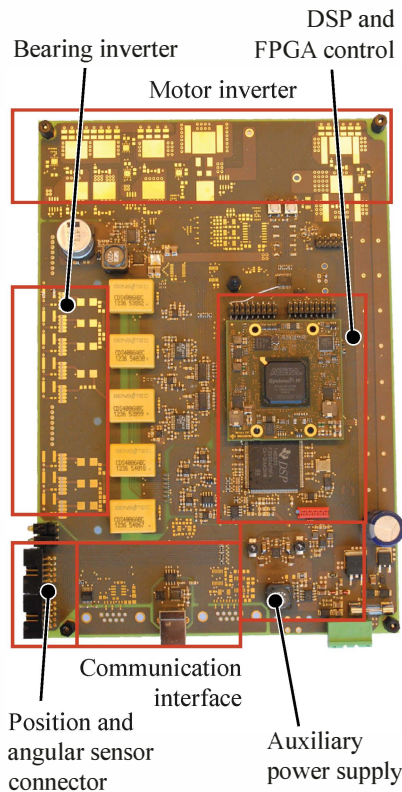


Figure 10: Power and control electronics to drive and control novel dual hetero-/homopolar, slotless, self-bearing, permanent-magnet synchronous motor reaction wheel demonstrator.

B. Measurements

The PCB based eddy current displacement sensors have been tested together with the demodulation electronics and the RW demonstrator rotor. The signals for a displacement in x-direction (Figure 11) and y-direction (Figure 12) show a good linearity no cross coupling between x-displacement and y-measurement and vice versa, and have a resolution of about 1 to 2 μm . The next steps in the experimental verification will be the closure of the current control loop, and the position control loop subsequently.

V. CONCLUSIONS

Smaller satellites require smaller angular momentum (L) reaction wheels (RWs), which results in lower angular momentum density (L/m), especially if the speed is limited as with ball bearings. The only way to increase L/m is to increase the rotational speed, use high strength materials for the inertia disks, and operate closer to or at the stress limit of these materials. Active magnetic bearings are the only alternative for higher rotational speeds and vacuum requirement.

Scaling law comparison of active magnetic bearing RWs and ball bearing RWs shows that above an angular momentum of 0.05 Nms magnetic bearing RWs perform better (higher L/m) but at a much higher maximum power demand.

A novel dual hetero-/homopolar, slotless, self-bearing, permanent-magnet synchronous machine concept has been presented. The application of forces and torque is

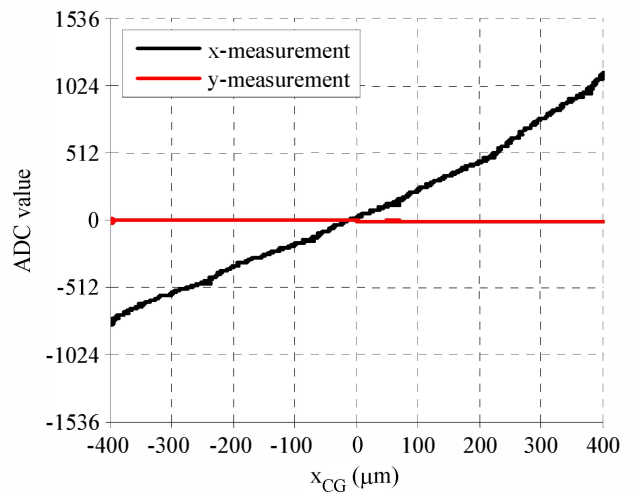


Figure 11: Radial rotor position measurement obtained by the PCB eddy current displacement sensor: Radial rotor position measurement when varying the rotor position x_{CG} ($y_{CG}=0$). The reference measurement is obtained by an external optical displacement sensor (Keyence LK-H022).

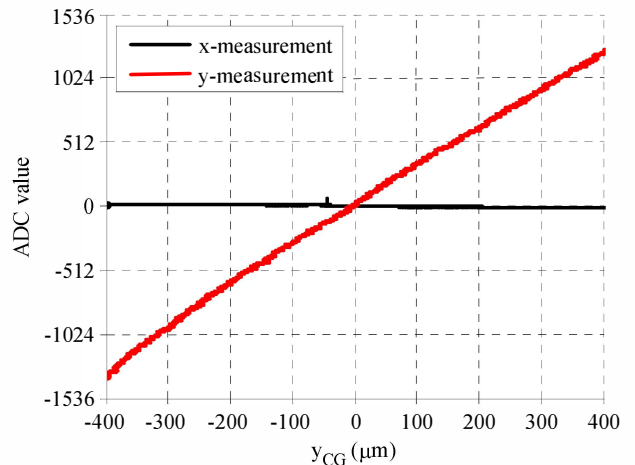


Figure 12: Radial rotor position measurement obtained by the PCB eddy current displacement sensor: Radial rotor position measurement when varying the rotor position y_{CG} ($x_{CG}=0$). The reference measurement is obtained by an external optical displacement sensor (Keyence LK-H022).

therefore divided up into two motors: Motor torque and radial bearing forces are applied in the heteropolar motor, axial and radial bearing forces are applied in the homopolar motor. All six-degrees of freedom are controlled actively.

The concept is ideally suited for minimizing the size of RWs or integrated power and attitude control systems (IPACS) for small satellites, as it allows for an increase in rotational speed and can run in vacuum, both not possible with today's state-of-the-art ball bearing RWs and IPACS. A RW demonstrator design has been presented for a rotational speed of 250 000 rpm. The demonstrator is realized in hardware and ready for experimental verification.

In the current implementation of the self-bearing RW demonstrator, the mass of the total system is at least ten times the mass of the rotor. This means the mass

overhead is considerable. This is a consequence of the additional components such as the bearing windings, the bearing power electronics, the rotor position sensor and the control electronics. If this mass overhead can be reduced, the magnetically levitated RW becomes even more competitive compared to RWs employing ball bearings. Therefore, future research has to be focused on a higher integration of system components such as the integration of bearing windings and rotor position sensor (self-sensing magnetic bearing).

REFERENCES

- [1] R. Varatharajoo and R. Kahle, "A review of conventional and synergistic systems for small satellites," *Aircraft Engineering and Aerospace Technology*, vol. 77, no. 2, pp. 131–141, 2005.
- [2] M. Scharfe, T. Roschke, E. Bindl, D. Blonski, "Design And Development Of A Compact Magnetic Bearing Momentum Wheel For Micro And Small Satellites", *Conference on small satellites*, 2001.
- [3] W. Ley, K. Wittmann and W. Hallmann, *Handbook of Space Technology*. John Wiley & Sons, 2009.
- [4] R. Votel and D. Sinclair, "Comparison of control moment gyros and reaction wheels for small earth-observing satellites," *Proceedings of the AIAA/USU Conference on Small Satellites*, SSC12-X-1, 2012.
- [5] C. Zwyssig, J. W. Kolar, and S. Round, "Megaspeed drive systems: Pushing beyond 1 million r/min," *IEEE/ASME Transactions on Mechatronics*, vol. 14, no. 5, pp. 564–574, Oct. 2009.
- [6] J. Fausz, B. Wilson, C. Hall, D. Richie, and V. Lappas, "Survey of technology developments in flywheel attitude control and energy storage systems," *Journal of Guidance, Control, and Dynamics*, vol. 32, no. 2, pp. 354–365, 2009.
- [7] T. Baumgartner, R. Burkart, and J. W. Kolar, "Analysis and Design of a 300-W 500 000-r/min Slotless Self-Bearing Permanent-Magnet Motor," *IEEE Transactions on Industrial Electronics*, Vol. 61, No. 8, pp. 4326–4336, August 2014.
- [8] Online: <http://www.astrofein.com/astro-und-feinwerktechnik-adlershof/produkte/raumfahrt-eng/8/reaktionsraeder/>
- [9] D. Steinert, T. Nussbaumer, J. W. Kolar, "Concept of a 150 krpm Bearingless Slotless Disc Drive with Combined Windings," *Proceedings of the IEEE International Electric Machines and Drives Conference (IEMDC 2013)*, Chicago, USA, May 12–15, 2013.
- [10] H. Mitterhofer and W. Amrhein, "Design aspects and test results of a high speed bearingless drive," in *Proceedings of the 9th IEEE International Conference on Power Electronics and Drive Systems (PEDS 2011)*, Dec. 2011, pp. 705–710.
- [11] A. Muesing, C. Zingerli, P. Imoberdorf, and J. W. Kolar, "PEEC based numerical optimization of compact radial position sensors for active magnetic bearings," in *Proceedings of the 5th IEEE International Conference on Integrated Power Systems (CIPS 2008)*, March 2008, pp. 1–5.
- [12] A. Looser, T. Baumgartner, J. W. Kolar, and C. Zwyssig, "Analysis and measurement of three-dimensional torque and forces for slotless permanent-magnet motors," *IEEE Transactions on Industry Applications*, vol. 48, no. 4, pp. 1258–1266, July–Aug. 2012.
- [13] T. Baumgartner and J. W. Kolar, "Multivariable state feedback control of a 500 000 rpm self-bearing motor," in *Proc. IEEE IEMDC*, May 2013, pp. 347–353.